RESEARCH ARTICLE

Unraveling enigmatic disjunctions: Population genetic analysis points to independent origins of rare rhododendrons in the *Rhododendron keiskei* complex (Ericaceae)

Shota Sakaguchi,[1] Hee-Joo Choi,[2] Watanabe Yoichi,[3] Daiki Takahashi,[4] Shun K. Hirota,[5] Masayuki Maki,[6] Shoki Murakami,[6] Taichi Harada,[6] Nobuo Kobayashi,[7] Yuji Kurashige,[8] Jun-Ho Song,[9] Hyeok-Jae Choi[10] & Seung-Chul Kim[2]

1 *Graduate School of Human and Environmental Studies, Kyoto University, Kyoto, 606-8501, Japan*
2 *Department of Biological Sciences, Sungkyunkwan University, South Korea*
3 *Graduate School of Horticulture, Chiba University, Japan*
4 *Faculty of Agriculture, Kyushu University, Kyushu University, Japan*
5 *Botanical Gardens, Osaka Metropolitan University, Japan*
6 *Graduate School of Life Sciences, Tohoku University, Japan*
7 *Faculty of Life and Environmental Science, Shimane University, Japan*
8 *Niigata Prefectural Botanical Garden, Japan*
9 *Department of Biology, Chungbuk National University, South Korea*
10 *Department of Biology & Chemistry, College of Natural Sciences, Changwon National University, South Korea*

Addresses for correspondence: Shota Sakaguchi, *sakaguchi.shota.6a@kyoto-u.ac.jp*; Hyeok-Jae Choi, *hjchoi1975@changwon.ac.kr*; Seung Chul Kim, *sonchus96@skku.edu*
The first two authors contributed equally.

DOI https://doi.org/10.1002/tax.13288

Abstract Unraveling species boundaries is pivotal for evolutionary biology and conservation endeavors. However, it proves challenging in instances where recent speciation is intertwined with complex demographic histories and natural selection processes. The *Rhododendron keiskei* complex, an evergreen rhododendron distributed in East Asia, consists of a widespread variety (*R. keiskei* var. *keiskei*) and a more restricted *R. keiskei* var. *hypoglaucum*. Intriguingly, the latter is exceptionally rare yet displays a disjunction that spans approximately 1100 km. This study aimed to elucidate the evolutionary backgrounds of the enigmatic disjunctions of *R. keiskei* var. *hypoglaucum* and to propose species delimitation within the species complex. An integrative approach, combining genomic data (MIG-seq and GBS-derived SNPs) with Scanning Electron Microscopy analysis of leaf microstructures was adopted in this study. Phylogenetic analyses revealed significant divergence among the studied rhododendrons. Genetic demographic analyses favored the population models that assumed non-monophyly of two disjunct populations of *R. keiskei* var. *hypoglaucum* indicating their independent origins. Recent gene flow between the widespread *R. keiskei* var. *keiskei* and "var. *hypoglaucum*" populations were limited due to geographic and habitat isolation factors, even in areas where their distributions overlap. Detailed morphological assessments detected distinctions between morphologically similar "var. *hypoglaucum*" populations based on leaf microstructures and flowering habits. Our study has shown that the apparent disjunctions of rare rhododendrons are more likely attributed to morphological convergence, possibly due to similar environmental selections in unrelated taxa. The finding highlights the importance of an integrative approach for resolving taxonomic challenges in plant species complexes.

Keywords demographic modeling; disjunct distribution; East Asia; endangered species; phylogeny; species delimitation

Supporting Information may be found online in the Supporting Information section at the end of the article.

■ INTRODUCTION

Species delimitation is the act of identifying species-level biological diversity through the recognition of evolutionary patterns (Carstens & al., 2013). Identifying species is essential for understanding the evolutionary history of a species group and allocating resources for biological conservation (Fraser & Bernatchez, 2001; Supple & Shapiro, 2018). However, attempting to categorize organisms into purely discrete units is a difficult task with differing opinions (Morrison, 2017). For the past century, different species concepts with alternative definitions have been proposed, which resulted in different conclusions concerning the boundaries and numbers of species. For example, the biological species concept is widely

Article history: Received: 22 Feb 2024 | returned for (first) revision: 8 Apr 2024 | (last) revision received: 6 Sep 2024 | accepted: 9 Sep 2024 | published online: 30 Nov 2024 | **Associate Editor:** Gulzar Khan |

adopted in evolutionary biology, requiring a species to be reproductively isolated from similar groups (Mayr, 1942). Nevertheless, it could be argued that controlled interbreeding does not provide evidence of species status (Mayr, 1963), and practically, applying this species concept to natural populations can be challenging due to the difficulty in obtaining data on the extent of reproductive isolation. The growing popularization of the phylogenetic species concept has led to a massive increase in species numbers in many animal taxa over the last two decades, mainly as a result of raising former subspecies to species rank (Zachos, 2015).

Despite such apparent differences in species concepts, alternative concepts agree in treating existence as a separately evolving metapopulation lineage as the primary defining property of species status (De Queiroz, 2007). This unified species concept considers the property as the only necessary definition of species and adopts additional properties acquired by lineages during speciation. Multiple lines of evidence from several properties that arise during lineage divergence can be interpreted as more robust support for the hypotheses of lineage separation. Under the unified concept, disagreements about species delimitation result from differences concerning the reliability of phylogenetic inference methods, the relevance of particular data, temporal scale, etc. Therefore, an integrative approach is necessary to better understand species boundaries because the complexity of species biology requires that species boundaries be studied from multiple, complementary perspectives (Dayrat, 2005). Such an approach is particularly essential for a species complex that recently diverged and shows complex phenotypes affected by demographic histories and natural selection processes.

Morphological data is traditionally the primary source for species delimitation but has some limits. First, an organism's morphology varies plastically in response to environmental differences, leading to the misidentification of environmentally induced variations as distinct species (Wu & al., 2023). Conversely, in recently radiating clades, reproductively isolated species may lack clear morphological differentiation (Padilla-García & al., 2018; Joffard & al., 2022). Morphology may not match phylogenetic signals when parallel trait evolution and genetic introgression occur in a related species group (Zhang & al., 2023; Wang & al., 2024). To better recognize the species boundaries, multiple sources of evidence derived from ecology, reproductive biology, genetics and geographic distribution patterns can be integrated with morphological data (Goldstein & DeSalle, 2011; Martínez-Domínguez & al., 2024). Notably, as obtaining DNA sequence data has become more accessible owing to the dramatically decreasing costs of generation of genomic data, genome-wide single nucleotide polymorphism (SNP) data are increasingly integrated into species delimitation. Such genomic data enables the reliable inference of complex evolutionary histories (Excoffier & al., 2021), deciphering divergence patterns under interspecific introgressions (Hedrick, 2009; Waples & al., 2018), and allowing hypothesis testing based on statistical models (Carstens & al., 2013; Yang, 2015; Hillis & al., 2021). Although genetic data will not solve the problem of discrete classification in an inherently non-discrete system, it can help to have a more complete understanding of the evolutionary dynamics during speciation (Supple & Shapiro, 2018).

Rhododendron keiskei Miq. (*R.* subg. *Rhododendron* subsect. *Triflora*, Ericaceae) is a medium-sized evergreen rhododendron with yellowish flowers distributed in the warm-temperate regions of the Japanese Archipelago (Pacific side of Central Honshu, Shikoku, Kyushu, and Yaku Isls.) (Yamazaki, 1996) (Fig. 1A,B). The species is found in shaded rocky places around the edges of mixed evergreen and deciduous forests. In 1932, the *R. keiskei* plants inhabiting dry and exposed rocky ridges of the Kanto District were described as *R. keiskei* var. *hypoglaucum* Suto & T.Suzuki, which show distinct morphological characteristics from *R. keiskei* var. *keiskei* (Suzuki, 1932) (Fig. 1C,E). The plants of *R. keiskei* var. *hypoglaucum* are smaller (<1 m) than *R. keiskei* var. *keiskei* (1–2 m) and have elliptic leaves with obtuse apex and glaucous beneath and white flowers with a yellowish tinge. The *R. keiskei* var. *hypoglaucum* populations are distributed in "edaphic islands" of isolated cherts and limestone outcrops, usually surrounded by *R. keiskei* var. *keiskei* populations. Since its description, *R. keiskei* var. *hypoglaucum* has long been believed to be a local endemic to Japan. However, in 2012, a yellowish-flowered *Rhododendron* population was discovered on a continental island off the southern Korean Peninsula (Fig. 1A). The Korean plant was characterized by evergreen and entire leaves with lepidote hairs and white flowers tinged with yellow (Fig. 1D). Based on the morphological similarity, the Korean *Rhododendron* was identified as *R. keiskei* var. *hypoglaucum* (Yang & al., 2015; Choi & al., 2022) (Fig. 1E). The occurrence of *R. keiskei* var. *hypoglaucum* on the Korean island was regarded as intriguing in terms of biogeography; the two regional populations are both small (consisting of less than 500 mature individuals) (Japanese Ministry of Environment, 2020) but show significant disjunct distributions ca. 1100 km away from each other. On the other hand, the habitat of the Korean *Rhododendron* was the coastal rocky slope, different from Japanese *R. keiskei* var. *hypoglaucum*, which is limited to inland mountain ridges. Also, we noticed that the number of flowers per inflorescence reported for the Korean population was larger (2–6) compared to Japanese *R. keiskei* var. *hypoglaucum* (1–2). Therefore, with the currently available information, it is unclear whether the Korean *Rhododendron* (hereafter, *Rhododendron* sp.) can be treated as *R. keiskei* var. *hypoglaucum*.

In this study, we aimed to provide an insight into the species delimitation of the *Rhododendron keiskei* complex by revealing the evolutionary backgrounds of the enigmatic disjunctions of "var. *hypoglaucum*" (i.e., Japanese *R. keiskei* var. *hypoglaucum* and Korean *Rhododendron* sp. populations). We have based our study on multiple data sources from two sets of genome-wide markers (multiplexed inter-simple sequence repeat [ISSR] genotyping by sequencing [MIG-seq; Suyama & Matsuki, 2015] and genotyping by sequencing [GBS; Elshire & al., 2011]) and morphological assessment to

delineate the rhododendron species complex. First, phylogenetic and genetic demographic analyses were performed to test the hypothesis that *Rhododendron* sp. and *R. keiskei* var. *hypoglaucum* form a monophyletic group, asking whether they satisfy the property in the monophyletic version of the phylogenetic species concept (Donoghue, 1985; De Queiroz, 2007). Since gene genealogies can be affected by gene flow between lineages, the demographic analysis considered a series of alternative models that accounted for various gene flow patterns. Secondly, we inferred divergence times and changes in effective population size to reconstruct the historical biogeography of the species complex. During the Pleistocene era, the Japanese Islands were intermittently connected to and isolated from the Eurasian continent (Kimura, 1996). These geological events provided multiple opportunities for the ancestral lineage of *R. keiskei* to disperse and diverge across the sea channel between the current Korean Peninsula and the Japanese Islands. Therefore, determining the timing of divergence of Korean *Rhododendron* sp. from Japanese species is particularly important for understanding the role of land configurations in promoting plant speciation in this region. Specifically, based on the demographic parameters obtained, we tested whether *Rhododendron* sp. is descended from Japanese *R. keiskei* taxa that migrated via glacial land bridges repeatedly formed in the late Pleistocene (Fig. 2A,B) or if it represents a relict lineage with a long isolation history following migration via land bridges formed in the early Pleistocene (Kitamura & Kimoto, 2006). Lastly, we combined the results from genetic and detailed morphological assessments to propose a taxonomic rearrangement of the *Rhododendron keiskei* complex.

■ MATERIALS AND METHODS

Plant materials. — The plant materials analyzed in this study are summarized in suppl. Table S1 for morphological assessment, and suppl. Tables S2 and S3 for genetic analyses. The leaf materials of *Rhododendron keiskei* var. *keiskei* and *R. keiskei* var. *hypoglaucum* were collected from wild populations that cover the complete range of the taxa in Japan (Figs. 1A, 2A,B). Upon collection, the leaves were immediately dried using silica gel and kept in the dark at room temperature before DNA extraction. The *Rhododendron* sp. materials were provided by Korea National Arboretum, Daegu Arboretum, and Goseung Plant Nursery. Note that we could not include *R. keiskei* var. *ozawae* T.Yamaz., a dwarf form variety of *R. keiskei* described from the summit area of Yaku Island, due to its natural rarity.

Genetic analyses. — The silica gel-dried leaf samples (approximately 1 cm^2) were pulverized with TissueLyser II (QIAGEN, Germany). After the polysaccharides were removed from the leaf powder with HEPES (4-(2-hydroxyethyl)-1-piperazineethanesulfonic acid) buffer (0.1 M, pH 8.0), total DNA was extracted using the cetyltrimethylammoniumbromide (CTAB) method (Murray & Thompson, 1980).

The extracted DNA was used for constructing two types of genomic libraries for reduced representation sequencing: MIG-seq (Suyama & Matsuki, 2015) and GBS (Elshire & al., 2011). Briefly, MIG-seq uses the tailed and barcoded ISSR primers to amplify loci in a two-step PCR protocol, followed by size selection and sequencing on the Illumina platform. This method does not require the conventional steps of

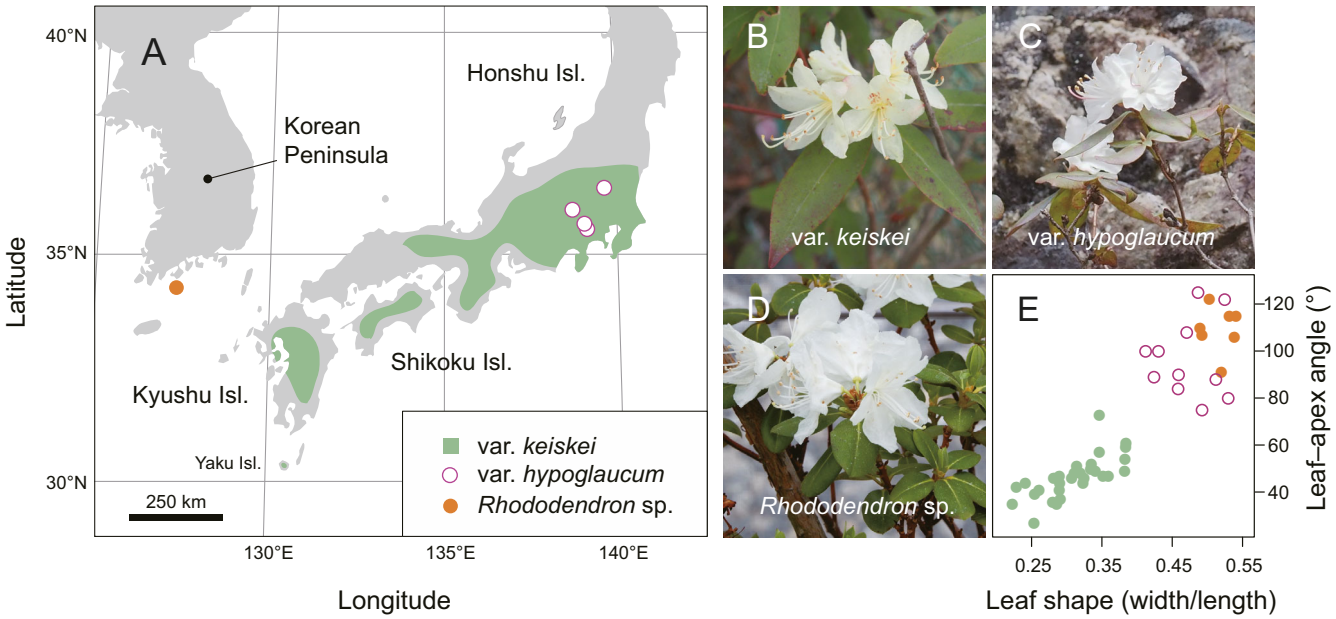

Fig. 1. A, The geographic distribution of the *Rhododendron keiskei* complex. **B–D**, Morphological comparisons of: **B**, *R. keiskei* var. *keiskei*; **C**, *R. keiskei* var. *hypoglaucum*; **D**, *Rhododendron* sp. **E**, Comparison of leaf blade morphology of three taxa, based on the voucher specimens (suppl. Table S1). Note that the leaf morphological variation of *R. keiskei* var. *hypoglaucum* and *Rhododendron* sp. overlap. — Photos: B, Shota Sakaguchi; C, Watanabe Yoichi; D, J.-C. Yang.

genomic DNA fragmentation and ligation of barcoded adapters, thus reducing the cost and labor associated with library preparations. The MIG-seq libraries were constructed for all the samples listed in suppl. Table S2 based on the protocol in Suyama & Matsuki (2015), with a slight modification of altering the annealing temperature from 48°C to 38°C in the first PCR (Suyama & al., 2022). The amplicons were purified and sequenced using MiSeq Reagent Kit v.3 (150 cycles) on an Illumina MiSeq Sequencer (Illumina, San Diego, California, U.S.A.). We skipped sequencing the first 17 bases of read 1 and 2 (simple sequence repeat primer regions and anchors) using "DarkCycle".

While MIG-seq has been effectively applied to many population genetic studies to date, the number of SNP markers obtained by this method ranges from hundreds to a few thousand (Suyama & Matsuki, 2015), which is fewer than those produced by other methods (e.g., RAD-seq). To validate the genetic statistics inferred by MIG-seq markers, we prepared GBS libraries for population samples to obtain more genetic markers. These included 52 samples for *Rhododendron keiskei* var. *keiskei*, 21 samples for *R. keiskei* var. *hypoglaucum* in Japan, and 8 for *Rhododendron* sp. (suppl. Table S3). Libraries were prepared by the restriction enzyme digestion of DNA with *Msp*1 and *Pst*1, followed by ligation of barcoded adapters according to a protocol modified by Elshire & al. (2011). The pooled libraries were sequenced on an Illumina HiSeq X system (Illumina) with an average 151 bp length for paired-end reads. Two sequencing runs were conducted consecutively.

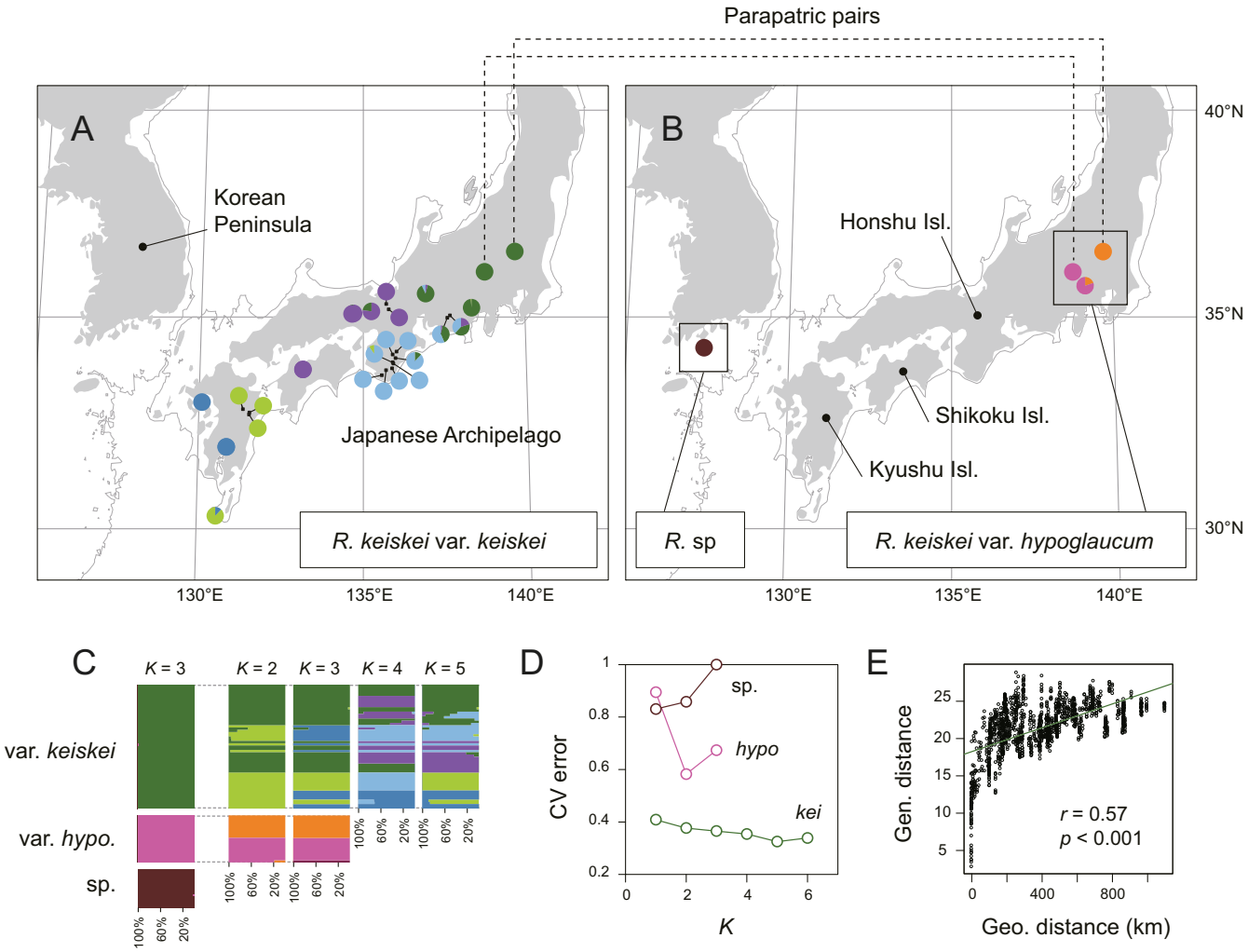

Fig. 2. A & B, The pie charts illustrate the genetic ancestry inferred by ADMIXTURE analysis (the clustering patterns at $K = 5$ for *Rhododendron keiskei* var. *keiskei*, $K = 2$ for *R. keiskei* var. *hypoglaucum*, and $K = 1$ for *Rhododendron* sp. are shown). The exposed sea floor during the last glacial maximum (ca. 21,000 years ago) is illustrated as a gray line; **C**, The individual genetic ancestry inferred by ADMIXTURE program is shown as horizontal bar plots. The leftmost graph shows the clustering pattern estimated from the genotype data of three taxa ($K = 3$). For the two taxa with multiple populations analyzed, the results of ADMIXTURE clustering performed for each taxon are shown from $K = 2$ to $K = 5$ for *R. keiskei* var. *keiskei* and at $K = 2$ and $K = 3$ for *R. keiskei* var. *hypoglaucum*. The individuals are ordered based on their geographical locations of origin; **D**, Changes of cross-validation (CV) error as a function of the number of genetic clusters (K) are shown; **E**, Isolation by distance (Nei's genetic vs. geographical) plot for *R. keiskei* var. *keiskei*.

Read processing and genotype calling. — For the MIG-seq reads, low-quality bases were trimmed using Trimmomatic v.0.39 (Bolger & al., 2014), with the following options: HEADCROP = 6, MINLEN = 71, ILLUMINACLIP:2:30:10. The GBS raw reads were demultiplexed using barcode sequences associated with each sample to generate separate FASTQ files for all 81 samples. Adapter sequences were removed using Cutadapt v.1.8.3 (Martin, 2011), and the demultiplexed reads were trimmed using DynamicTrim (phred score ≥ 20) and LengthSort (short read length ≥ 25 bp) in SolexaQA v.1.13 (Cox & al., 2010). Poor-quality sequences with Phred quality scores below Q = 20 (or an error probability of 0.05) were removed, and short read lengths of <25 bases were discarded.

The *denovo_map* pipeline in Stacks2 (Rochette & al., 2019) was used to assemble cleaned MIG-seq and GBS reads, respectively. The pipeline clusters the reads into loci within samples using *ustacks* and loci into stacks between samples using *cstacks* and *sstacks*. The assembly uses nucleotide mismatches for clustering and allows reads to contain indels. We set the number of mismatches allowed between stacks within individuals (-M) and the number of mismatches allowed between stacks between individuals (-n) to 3. The SNP markers were exported using the *populations* pipeline in Stacks2. Potential paralogous and erroneous loci were filtered out based on the observed heterozygosity ($H_o > 0.5$) and minor allele frequency (<0.01). The markers with a relatively high missing rate (>0.10) were also filtered out.

In this study, we generated six different SNP datasets using Stacks2. The first set was prepared for inter-subgenera phylogeny and included the MIG-seq reads from 2 to 4 samples from three ingroup taxa (consisting of the *R. keiskei* complex) and three outgroup species, i.e., *Rhododendron mucronulatum* Turcz. (subg. *Rhododendron*), *R. albrechtii* Maxim. and *R. nipponicum* Matsum. (subg. *Pentanthera*). The second MIG-seq dataset was assembled for phylogenetic inference within *R.* subg. *Rhododendron* and included the *R. keiskei* complex and *R. mucronulatum*. The third to sixth MIG-seq datasets were produced for population genetic analyses and included all the *R. keiskei* complex samples listed in suppl. Table S2 ($n = 93$), i.e., all the *R. keiskei* var. *keiskei* samples ($n = 55$), var. *hypoglaucum* samples ($n = 21$) and *Rhododendron* sp. samples ($n = 17$), respectively. The seventh dataset, created from the GBS-derived reads for population genetic analysis, consisted of 81 samples of three *R. keiskei* taxa (suppl. Table S3).

Phylogenetic tree inference. — To infer the rooted phylogenetic tree for the sequenced *Rhododendron* species, the MIG-seq SNPs that are fixed within and variable among species were extracted from the first dataset. The best nucleotide substitution model for the SNP-only data was selected using ModelFinder (Kalyaanamoorthy & al., 2017), implemented in IQ-TREE v.2.2.5 (Minh & al., 2020). The maximum likelihood (ML) tree search was performed with 1000 ultrafast bootstrap replicates (Hoang & al., 2017), using IQ-TREE v.2.2.5. We also constructed the ML tree for *R.* subg. *Rhododendron* with *R. mucronulatum* as an outgroup, for which the MIG-seq SNPs that are polymorphic within species were included to increase the amount of data. An unrooted ML tree was constructed similarly for the GBS-derived SNPs (seventh dataset).

Population genetic analyses. — Summary statistics of genetic diversity (number of polymorphic sites, nucleotide diversity, heterozygosity) and differentiation index (F'_{ST}) were calculated for the ingroup taxa based on the third and seventh datasets, using the *populations* program implemented in Stacks2. To detect the population structure within the *Rhododendron keiskei* complex, we employed the ADMIXTURE program (v.1.3.0) (Alexander & al., 2009), which applies the same population model as STRUCTURE (Pritchard & al., 2000) to multilocus SNP genotype datasets. The number of clusters (K) was set from $K = 1, \ldots,10$ for the three-taxon dataset. We subsequently performed ADMIXTURE analyses for each taxon, assuming the maximum number of $K = 6$ for *R. keiskei* var. *keiskei* and $K = 3$ for *R. keiskei* var. *hypoglaucum* and *Rhododendron* sp. Cross-validation (CV) error was calculated to identify the values of K, for which the model has the best predictive accuracy.

Isolation by distance was tested for the wide-ranging taxon of *Rhododendron keiskei* var. *keiskei* using Mantel's test (999 permutations) implemented in the R *vegan* package (Oksanen & al., 2012) in R v.3.5 (R Development Core Team, 2018).

Demographic inferences. — A demographic modeling approach was employed to investigate the evolutionary scenarios that can account for the observed genetic variations of the *Rhododendron keiskei* complex. For this analysis, three *Rhododendron* populations (*R. keiskei* var. *keiskei*, var. *hypoglaucum*, and *Rhododendron* sp.) were considered to fuse each other at historical times into an ancestral population when looking backward in time. The assumption was made that *R. keiskei* var. *hypoglaucum* split first in topology T1, var. *keiskei* in topology T2, or *Rhododendron* sp. in topology T3, respectively (see Fig. 4A). Topology 2 represents a monophyletic group consisting of *R. keiskei* var. *hypoglaucum* and *Rhododendron* sp., consistent with the taxonomic assignment of *Rhododendron* sp. by Yang & al. (2015). The two other topologies indicate non-monophyly of *R. keiskei* var. *hypoglaucum* and *Rhododendron* sp. Gene flow among *R. keiskei* var. *keiskei*, var. *hypoglaucum*, and *Rhododendron* sp. with various combinations was assumed. As a result, 24 alternative demographic models were generated, as illustrated in Fig. 4B.

In these models, each current and ancestral population was assumed to have distinct population sizes, and the strength of gene flow was allowed to vary between population pairs. Priors for population size in haploid numbers were set as unif[1×10^3, 1×10^6], except for the widespread *Rhododendron keiskei* var. *keiskei* (unif[1×10^4, 1×10^7]). The time priors for the most recent divergence in a number of generations were considered as unif[1×10^3, 1×10^6], and the time differences (ΔT) from the most recent divergence were defined to have unif[1×10^3, 1×10^6] priors. Priors for

migration rate parameter were set as the effective number of migrants per generation following unif[1×10^{-2}, 20]. Migration between the two highly disjunct taxa of *R. keiskei* var. *hypoglaucum* and *Rhododendron* sp. were assumed to occur only before a historical time of T(m) that was set to follow unif[1×10^{3}, 1×10^{6}]. In the presence of missing values, the site frequency spectra were constructed by the down-projection method implemented in the easySFS program (https://github.com/isaacovercast/easySFS). To do so, easySFS projects down a genetic data matrix to a smaller sample size and averages over all possible resamplings to construct a complete data matrix. The folded site frequency spectra were estimated from the second SNP dataset, with projection values specified as 25 for *R. keiskei* var. *keiskei*, 18 for var. *hypoglaucum*, 14 for *Rhododendron* sp., depending on sample size. Fastsimcoal2 v.2.6 (Excoffier & al., 2021) was run 100 times to fit each demographic model to the observed spectrums and estimate the maximum composite likelihood parameter values with the following options: -n10000 -m -M -L50. For the demographic model with the lowest Akaike information criterion (AIC) value, 100 parametric bootstrap analyses were performed to obtain confidence intervals of demographic parameters. The original parameter values were converted to absolute scale assuming a generation time of 10 years (Yoichi & al., 2021; Zhang & al., 2021) and a mutation rate of 1.0×10^{-8} per site per generation, which is moderate for seed plants (Ossowski & al., 2010; Schmid-Siegert & al., 2017; Hofmeister & al., 2020).

Historical changes in effective population size were estimated for each taxon of the *Rododendron keiskei* complex. One-dimensional site frequency spectrums were estimated by easySFS based on the fourth to sixth datasets. The projection values were specified as 45 for *R. keiskei* var. *keiskei*, 18 for var. *hypoglaucum*, 14 for *Rhododendron* sp., depending on each sample size. The resultant spectra were used as inputs for Stairway Plot 2 (Liu & Fu, 2020). The parameter conversion utilized the same generation time and mutation rate values as in the fastsimcoal2 analysis.

Evaluation of overall leaf shape. — Sixty-six voucher specimens were used to evaluate overall leaf shape, including 30 vouchers for *Rododendron keiskei* var. *keiskei*, 11 for var. *hypoglaucum*, and 7 for *Rhododendron* sp. (suppl. Table S1). Measurements were taken from scanned voucher images using ImageJ v.1.47 software (Abràmoff & al., 2004). One fully expanded leaf from each specimen was selected to measure the maximum length and width of the leaf blade, petiole length, and apex angle.

Morphological and cuticular micromorphological analyses. — All dried leaf samples were examined using a stereomicroscope to select healthy and dust off the mature leaves (Stereozoom S9D, Leica, Wetzlar, Germany). For the observations using a field-emission scanning electron microscope, selected clean mature leaves (*Rhododendron keiskei* var. *keiskei*, population IDs: SS1663, SS1664; *R. keiskei* var. *hypoglaucum*, IDs: SS1665, SS1666; *Rhododendron* sp., IDs: SS1423, SS1424; suppl. Table S2) were mounted on aluminum stubs using a double-sided adhesive conductive carbon disk (05073-BA, SPI Supplies, West Chester, Pennsylvania, U.S.A.). All samples were gold-coated using an ion-sputtering device (Q150T ES Plus, Quorum, East Sussex, U.K.) and observed using a field emission-scanning electron microscope (Zeiss Ultra Plus, Carl Zeiss, Jena, Germany) at an accelerating voltage of 5–10 kV and a working distance of 5–10 mm. The obtained quantitative characters were determined using the Digimizer software (Digimizer v.5.7.5, MedCalc Software [https://www.medcalc.org/], Belgium).

■ RESULTS

Phylogenetic relationship among *Rhododendron* species. — The genotype data for two subgenera (*Rhododendron* subg. *Rhododendron* and subg. *Pentanthera*) consisted of 763 SNPs with a mean coverage of ×32.0 per sample. The ML tree constructed from this dataset (Fig. 3A) shows that the *Rhododendron keiskei* complex formed a monophyletic group with relatively low bootstrap support (BS = 55%). When the phylogenetic inference was based on the SNP matrix (344 SNPs with a mean coverage of ×33.9) for the *R.* subg. *Rhododendron* (Fig. 3B), the monophyly of the species complex was strongly supported (BS = 100%). In this tree, *R. keiskei* var. *hypoglaucum* was inferred to have diverged initially, followed by the split of *R. keiskei* var. *keiskei* and *Rhododendron* sp. The taxa of *R. keiskei* var. *hypoglaucum* and *Rhododendron* sp. were not the closest relatives in either tree. The widespread taxon of *R. keiskei* var. *keiskei* included multiple subclades, while the two narrow-ranging taxa of *R. keiskei* var. *hypoglaucum* and *Rhododendron* sp. consisted of a few subclades (Fig. 3B). The unrooted ML tree based on GBS data suggested that *R. keiskei* var. *hypoglaucum* and *Rhododendron* sp. formed distinct clades separate from the *R. keiskei* var. *keiskei* clade (Fig. 3C).

Population genetic structure and genetic diversity. — The CV error in the ADMIXTURE analysis of the *Rhododendron keiskei* complex rapidly decreased from 0.33 at $K = 2$ to 0.23 at $K = 3$, and then reached a plateau around 0.20. Therefore, we considered that the clustering at $K = 3$ can capture the uppermost genetic structure within the species complex. The genetic clusters at $K = 3$ corresponded to the taxonomic entities of *R. keiskei* var. *keiskei*, var. *hypoglaucum*, and *Rhododendron* sp. (Figs. 2C, 3B). To investigate the genetic structure within each taxon, we performed ADMIXTURE analyses on SNP matrices assembled separately for each taxon. The patterns of CV error change (Fig. 2D) indicated that $K = 1$ for *Rhododendron* sp., $K = 2$ for *R. keiskei* var. *hypoglaucum*, and $K = 5$ for *R. keiskei* var. *keiskei* are the appropriate numbers of clusters for each taxon. The genetic differentiation within *R. keiskei* var. *keiskei* was significantly associated with geography ($r = 0.57$, $p < 0.001$ in Mantel's test; Fig. 2E). The three populations of *R. keiskei* var. *hypoglaucum* were assigned to two genetic clusters (pink and orange clusters in Fig. 2B). Within the same mountain ranges, the parapatric

pairs of *R. keiskei* var. *keiskei* and var. *hypoglaucum* populations did not show any signatures of recent genetic admixture (Fig. 2A,B).

The genetic diversity of each *Rhododendron* taxon was assessed by MIG-seq and GBS-derived SNPs, respectively (Table 1). The genotyping rates per each taxon were high for both datasets, which ranged from 94.8% for *R. keiskei* var. *keiskei* to 98.3% for *Rhododendron* sp. in MIG-seq and from 94.0% for *R. keiskei* var. *keiskei* to 98.2% for *Rhododendron* sp. in GBS, respectively. Nucleotide diversity (pi) and expected heterozygosity (H_e) were highest in the wide-ranging *R. keiskei* var. *keiskei* (pi = 0.0040, H_e = 0.128), followed by var. *hypoglaucum* (pi = 0.0010, H_e = 0.023) and *Rhododendron* sp. (pi = 0.0009, *He* = 0.020), when MIG-seq data was used. The two taxa of *R. keiskei* var. *keiskei* and var. *hypoglaucum* showed tendencies of heterozygosity deficit (Table 1), probably due to intra-taxon population structures (Fig. 2C). Genetic differentiation among the three taxa was fairly high; F'_{ST} = 0.335 between *R. keiskei* var. *keiskei* and *Rhododendron* sp., 0.537 between *R. keiskei* var. *keiskei* and var. *hypoglaucum*, and

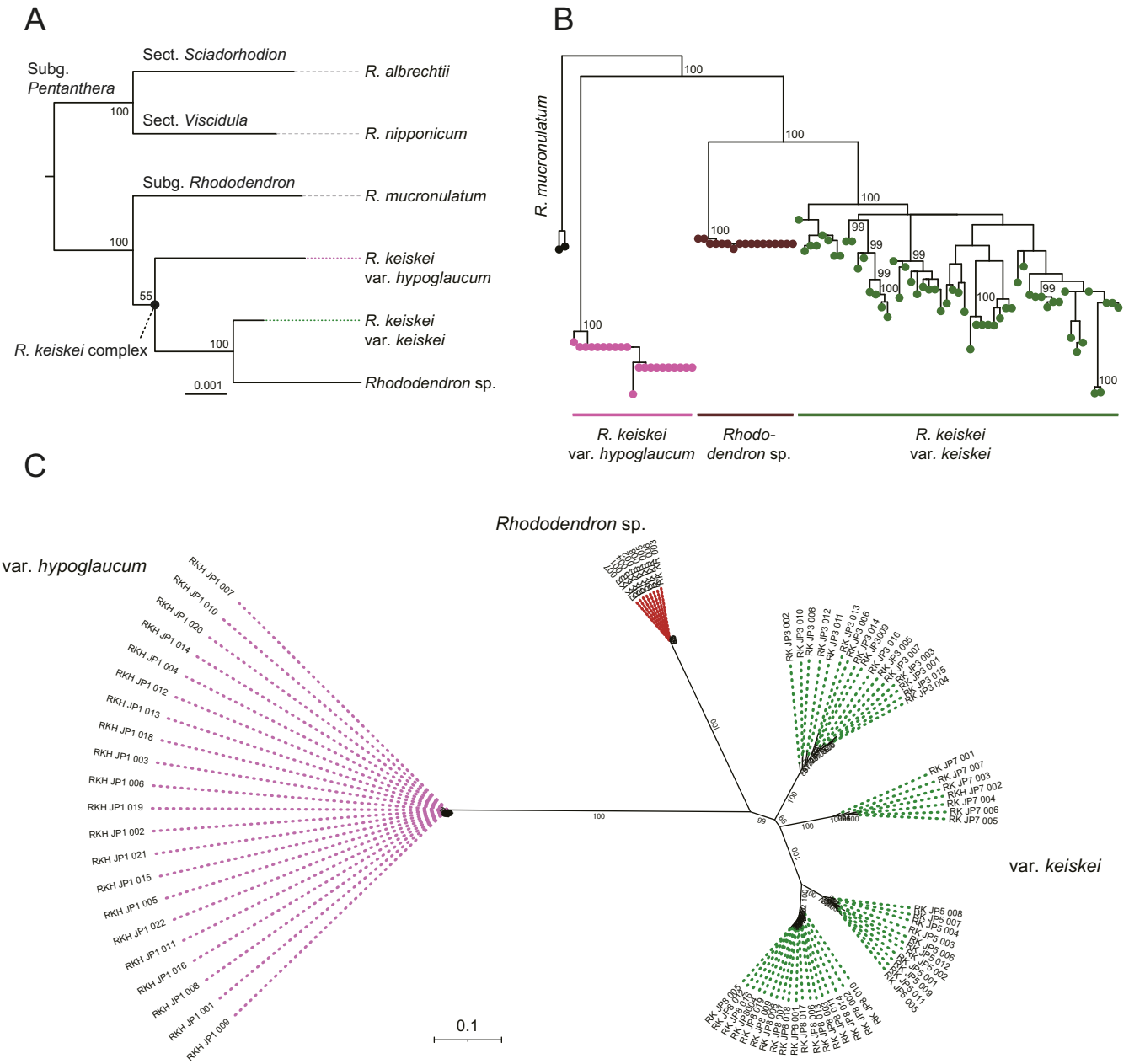

Fig. 3. The maximum likelihood trees based on MIG-seq data for the six *Rhododendron* taxa from: **A**, *R.* subg. *Rhododendron* and subg. *Pentanthera*, and **B**, for the *R. keiskei* complex with *R. mucronulatum* as an outgroup. The pie charts at the branch tips show the genetic ancestry of each sample, as estimated by ADMIXTURE analysis (corresponding to Fig. 2C). **C**, The unrooted maximum likelihood tree based on GBS data for the *R. keiskei* complex. — Bootstrap values are shown along the tree branches.

0.822 between *R. keiskei* var. *hypoglaucum* and *Rhododendron* sp. Nucleotide diversity (pi) and expected heterozygosity (H_e) based on the GBS data were highest in the wide-ranging *R. keiskei* var. *keiskei* (pi = 0.0641, H_e = 0.061), followed by var. *hypoglaucum* (pi = 0.0080, H_e = 0.008) and *Rhododendron* sp. (pi = 0.0074, H_e = 0.007). Genetic differentiation among the three taxa based on the GBS data was also high; F'_{ST} = 0.679 between *R. keiskei* var. *keiskei* and *Rhododendron* sp., 0.761 between *R. keiskei* var. *keiskei* and var. *hypoglaucum*, and 0.939 between *R. keiskei* var. *hypoglaucum* and *Rhododendron* sp. The average genetic differentiation among populations of *R. keiskei* var. *keiskei* was 0.352.

Historical demography. — The demographic models with topology T1 (Fig. 4A) tended to show lower AIC values than those with other topologies (Fig. 4B). The AIC values of the models assuming the monophyly of *Rhododendron keiskei* var. *hypoglaucum* and *Rhododendron* sp. (topology T2) were much larger than those of the models with topology T1 (ΔAIC >63, Fig. 4B). Among them, a model with topology T1 and gene flow terms of "*keiskei–hypoglaucum*" and "*hypoglaucum*–sp." attained the lowest AIC (7108.6), thus was considered as the best model. The second-best model (ΔAIC = 7.4) resembled the best model, albeit without incorporating gene flow terms between *R. keiskei* var. *hypoglaucum*

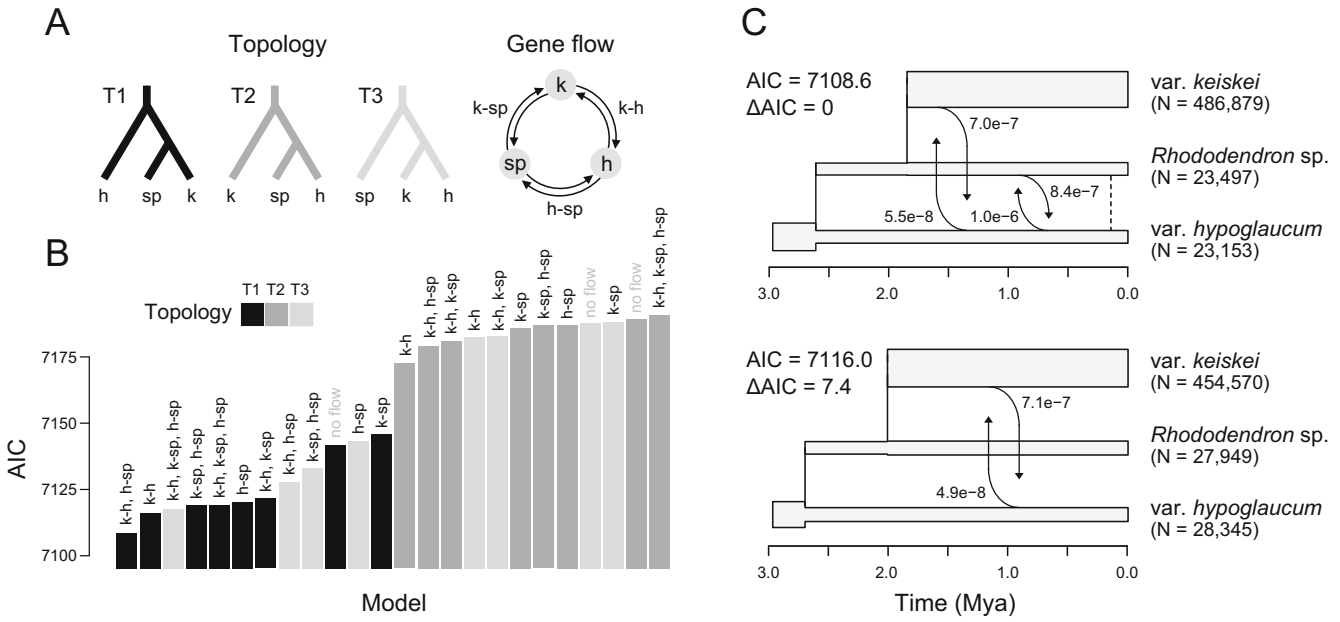

Fig. 4. A, Graphic representation of three different tree topologies and gene flow patterns assumed in demographic modeling of the three *Rhododendron* taxa. Each model was considered by combining different topologies and presence/absence of gene flow between populations. Abbreviations: h, *R. keiskei* var. *hypoglaucum*; k, *R. keiskei* var. *keiskei*; sp, *Rhododendron* sp. **B**, The AIC (Akaike information criterion) values for each demographic model are shown as bar plots. **C**, The best and second-best demographic models with associated demographic parameters are shown. The effective population size is shown as a haploid number, and the arrows indicate the migration rate backward in time. Abbreviation: Mya, million years ago.

Table 1. Summary statistics of genetic diversity estimated for each *Rhododendron* taxon, obtained from MIG-seq and GBS-derived SNPs, respectively.

Dataset/Taxon	No. samples analyzed	Genotyping rate	No. all sites	No. polymorphic sites (%)	pi (all sites)	H_e (variable sites)	H_o (variable sites)
MIG-seq							
R. keiskei var. *keiskei*	55	94.82%	16,744	575 (3.13%)	0.00404 (0.00097)	0.128 (0.015)	0.046 (0.002)
R. keiskei var. *hypoglaucum*	21	96.88%	77,882	264 (0.59%)	0.00101 (0.00020)	0.023 (0.005)	0.019 (0.005)
Rhododendron sp.	17	98.25%	82,867	74 (0.09%)	0.00088 (0.00023)	0.020 (0.005)	0.045 (0.010)
GBS							
R. keiskei var. *keiskei*	52	94.00%	2,249,420	1,793 (7.90%)	0.06406 (0.00026)	0.061 (0.001)	0.062 (0.001)
R. keiskei var. *hypoglaucum*	21	96.80%	1,735,237	210 (1.21%)	0.00804 (0.00003)	0.008 (0.001)	0.012 (0.001)
Rhododendron sp.	8	98.20%	2,131,417	163 (0.77%)	0.00742 (0.00003)	0.007 (0.001)	0.009 (0.001)

pi: nucleotide diversity, H_e: expected heterozygosity, H_o: observed heterozygosity.

and *Rhododendron* sp. Under the best model, the estimated effective population size of *R. keiskei* var. *keiskei* (N = 486,879 in haploid number) was more than 20 times larger than those of *R. keiskei* var. *hypoglaucum* (N = 23,153) and *Rhododendron* sp. (N = 23,497) (Fig. 4C, Table 2). The divergence time between the sister taxa of *R. keiskei* var. *keiskei* and *Rhododendron* sp. was estimated as 1.85 (1.65–1.99; 95% confidence interval [CI]) Mya, and the divergence of their ancestor and *R. keiskei* var. *hypoglaucum* was dated as 2.61 (2.14–4.67) Mya. The migration rate from *R. keiskei* var. *keiskei* to var. *hypoglaucum* was estimated as 1.13×10^{-6} (9.71×10^{-7}–1.90×10^{-6}) in forward time, and that of the opposite flow was 8.44×10^{-7} (4.87×10^{-7}–2.30×10^{-6}). The migration between *R. keiskei* var. *hypoglaucum* and *Rhododendron* sp. was inferred to have occurred until the late Pleistocene (0.14 [0.07–0.30; 95% CI] Mya). The divergence times and migration rates (between *R. keiskei* var. *keiskei* and var. *hypoglaucum*) were almost consistent between the best and second-best models (Fig. 4C).

The Stairway Plot analysis reconstructed a stable population size for *Rhododendron keiskei* var. *keiskei* after a demographic expansion since ca. 1 Mya (Fig. 5). The historical demography of the remaining two taxa appeared mostly stable, but the deficits of genetic polymorphisms in these taxa did not allow to estimate the size changes no longer than ca. 30 kya for *Rhododendron* sp. and ca. 300 kya for *R. keiskei* var. *hypoglaucum*.

Morphological assessments. — The epidermis cells of *Rhododendron keiskei* var. *hypoglaucum* were arranged regularly, while *R. keiskei* var. *keiskei* and *Rhododendron* sp. had irregularly arranged cells (Fig. 6). The mean length of stomata

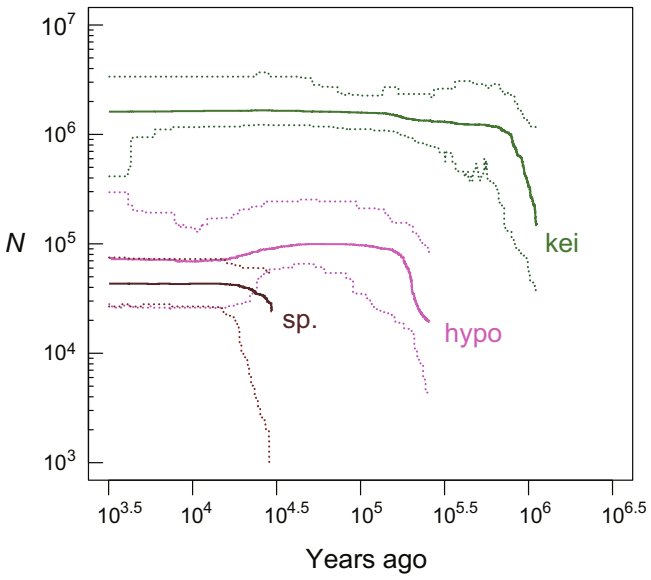

Fig. 5. The historical changes in effective population sizes (*N*) for the three *Rhododendron* taxa inferred by the Stairway Plot method. Abbreviations are: hypo, *R. keiskei* var. *hypoglaucum*; kei, *R. keiskei* var. *keiskei*; sp., *Rhododendron* sp. The solid and dotted lines indicate the median and 95% confidence intervals, respectively.

was 22.65 µm for *R. keiskei* var. *keiskei* and 20.34 µm for *R. keiskei* var. *hypoglaucum*, respectively, with an actinocytic type (Table 3). In contrast, *Rhododendron* sp. had smaller stomata (16.32 µm) than *R. keiskei* var. *keiskei* and var. *hypoglaucum*, with an anomocytic type. The gland scale density significantly differed among the three entities (Fig. 6), with 2.25/mm^2) for *R. keiskei* var. *keiskei*, 17.75/mm^2 for var. *hypoglaucum* and 33.15/mm^2 for *Rhododendron* sp. The mean scale diameter was largest in *R. keiskei* var. *keiskei* (208.87 µm), followed by *Rhododendron* sp. (181.65 µm) and *R. keiskei* var. *hypoglaucum* (158.99 µm) (Table 3). Abaxial epicuticular waxes were absent for *R. keiskei* var. *keiskei* and *Rhododendron* sp., while *R. keiskei* var. *hypoglaucum* had rods and filament types. *Rhododendron keiskei* var. *keiskei* had sparsely distributed adaxial multicellular glandular scales (0.37/mm^2). In contrast, *R. keiskei* var. *hypoglaucum* had moderately distributed (1.75/mm^2), and *Rhododendron* sp. had densely distributed multicellular glandular scales (5.87/mm^2) scales at higher densities (1.75/mm^2 and 5.87/mm^2, respectively) (Fig. 6, Table 3).

■ DISCUSSION

Origin of the small *Rhododendron* population on a continental island. — The evolutionary origin of the *Rhododendron* population on an island off the Korean Peninsula (*Rhododendron* sp.) was investigated by phylogenetic analyses and demographic modeling. The inferences from both approaches agreed that *Rhododendron* sp. was not most closely related to *R. keiskei* var. *hypoglaucum* despite their morphological resemblances (Figs. 3, 4). Instead, *Rhododendron* sp. was estimated to have diverged from the common ancestor with *R. keiskei* var. *keiskei* in the early Pleistocene (Table 2) after splitting from the *R. keiskei* var. *hypoglaucum* lineage. During the Pleistocene era, the Japanese Islands were connected to the Eurasian continent at ca. 2.0–1.3 Ma, except at 1.9 Ma when the southern current flowed into the Sea of Japan (Kitamura & Kimoto, 2006), and again during the glacial maxima of the late Pleistocene (Kimura, 1996) (Fig. 2A,B). These land connections are considered to have promoted plant and animal migrations across the regions (Sakaguchi & al., 2012; Honda & al., 2019). The divergence time of Korean *Rhododendron* sp. from *R. keiskei* var. *keiskei* in Japan was dated as 1.85 (1.65–1.99; 95% CI) Mya (Table 2), which roughly corresponds to the timing for the probable isolation of Japanese Islands from the continent. One possibility is that the ancestral lineage of *R. keiskei* var. *keiskei* and *Rhododendron* sp. migrated via the early Pleistocene land bridge to the Korean Peninsula, and subsequently, the two species allopatrically diverged when the channel was formed around 1.9 Mya (Kitamura & Kimoto, 2006). Our demographic analysis also revealed that *Rhododendron* sp. and *R. keiskei* var. *keiskei* have not exchanged genes significantly along their speciation event (Fig. 4C). This indicates that, despite the land connections by glacial dry land bridges in the

late Pleistocene, they appear to have been isolated on opposite sides of the channel, as estimated for other temperate plants that prefer mesic habitat (Qiu & al., 2009; Kikuchi & Osone, 2021).

We note that the divergence time estimates highly depend on the assumed generation time and mutation rate. Since precise demographic parameters are not available for the *Rhododendron keiskei* complex, we used the generation time of 10 years, which is the commonly used proxy of time to first flowering for shrubby rhododendrons (Yoichi & al., 2021; Zhang & al., 2021), and the mutation rate of 1.0×10^{-8} that falls within the estimates for vascular plants, including annuals and woody perennials (Ossowski & al., 2010; Schmid-Siegert & al., 2017; Hofmeister & al., 2020). However, the assumed values can differ somewhat from the actual parameters for this species complex. Also, the demographic models are oversimplified compared to the actual histories that organisms usually experience in the face of changing environments (Momigliano & al., 2021). Thus, it is essential to exercise caution when interpreting the scaled demographic parameters. Nonetheless, the estimated divergence time of *Rhododendron* sp. (ca. 1.85 Mya) was more than 10-fold older than the time frames of the two most recent glacial periods. Therefore, the hypothesis of *Rhododendron* sp. having been established by a recent dispersal of *R. keiskei* var. *hypoglaucum* from Japan can be safely rejected. The considerable level of population divergence ($F'_{ST} = 0.822$ in MIG-seq and 0.939 in GBS) between *Rhododendron* sp. and *R. keiskei* var. *hypoglaucum* is also suggestive of their long isolation histories, although they appear to have exchanged genes historically at very low rates (Fig. 4C).

Regarding character evolution, it is interesting that two rhododendrons (*Rhododendron keiskei* var. *hypoglaucum*, *Rhododendron* sp.) have generally similar leaf morphologies

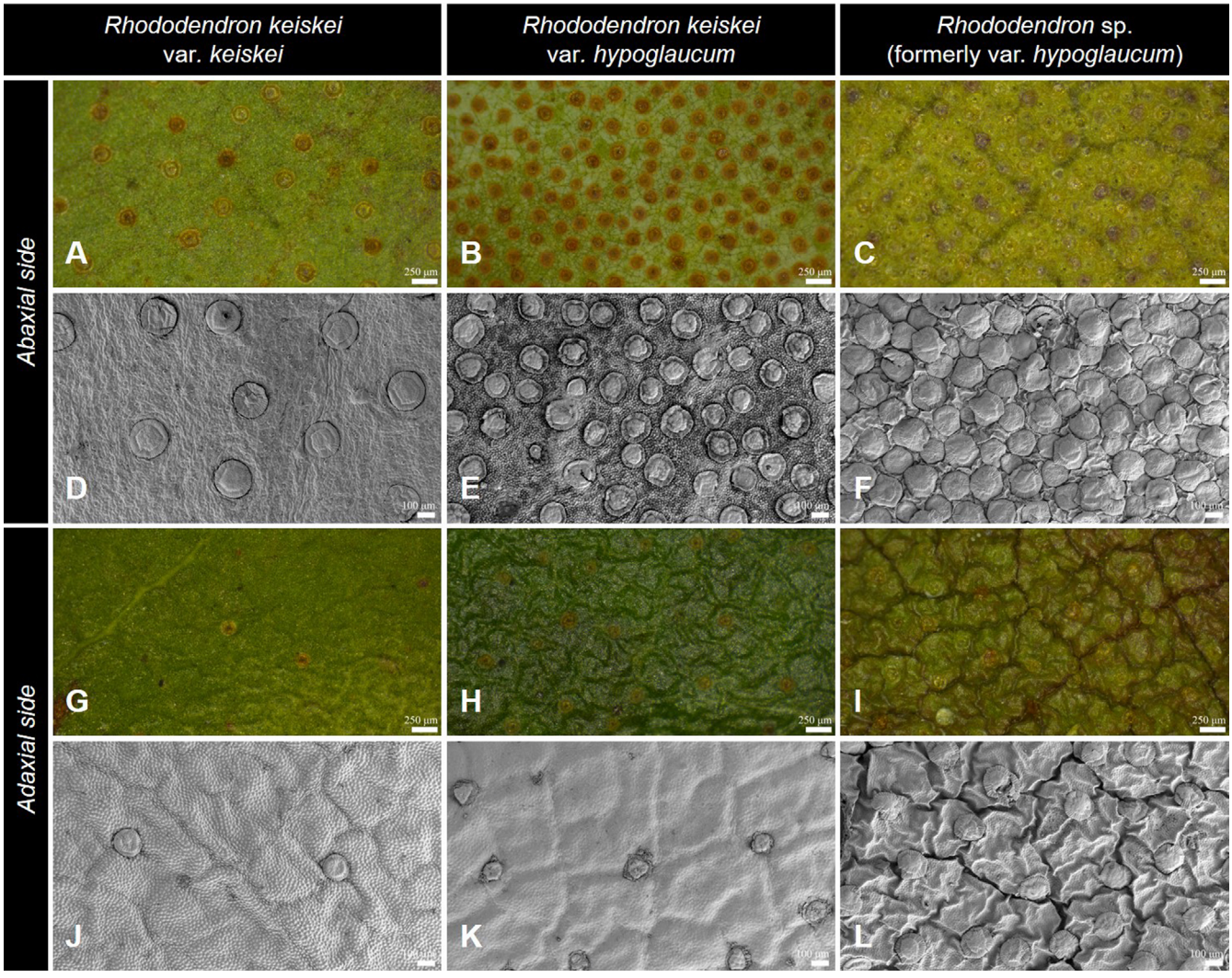

Fig. 6. Stereo and scanning electron micrographs of leaf surfaces of the three studied *Rhododendron* taxa. **A–C & G–I**, Stereo micrographs; **D–F & J–L**, Scanning electron micrographs. **A, D, G & J**, *Rhododendron keiskei* var. *keiskei*; **B, E, H & K**, *R. keiskei* var. *hypoglaucum*, **C, F, I & L**, *Rhododendron* sp. (formerly identified as *R. keiskei* var. *hypoglaucum*).

despite their probable independent origins. Given ancestral character states as seen in *R. keiskei* var. *keiskei*, one explanation may be that the solid leaves with a high density of scales may have evolved convergently in response to similar environmental selections (Schluter & Nagel, 1995; Roesti & al., 2014; Sakaguchi & al., 2018; Yoichi & al., 2018). The two taxa inhabit the more stressful and specialized habitats, that is, *R. keiskei* var. *hypoglaucum* in limestone/chert ridges and *Rhododendron* sp. in exposed coastal rocky slopes, respectively. Their leaf morphologies are likely adaptive in such dry and less fertile habitats (Poorter & al., 2009) and thus may have been selected in parallel in distant places. An alternative explanation posits that the leaf characteristics observed are retained from the common ancestor of the *R. keiskei* complex. According to this scenario, the thinner leaves of *R. keiskei* var. *keiskei* are considered a derived character state, which may have enabled *R. keiskei* var. *keiskei* to secondarily adapt to shady and mesic habitats. However, a reliable reconstruction of the ancestral character state based on phylogeny is hindered, as the phylogenetic analyses in this study do not include other members of *R*. subsect. *Triflora* species distributed in the southwestern part of China. To distinguish between these evolutionary scenarios, further efforts are needed to comprehensively reveal the phylogenetic relationships within *R*. subg. *Rhododendron*, including appropriate outgroup species from *R*. subsect. *Triflora*.

Table 2. Summary of the demographic parameters estimated for the best model. The best estimate and 95% confidence intervals (CI) are reported. The migration rate is reported as backward in time.

Parameter	Best estimate	2.5% CI	97.5% CI
N(k)	486,879	411,919	486,991
N(h)	23,153	17,732	27,428
N(sp)	23,497	17,521	26,523
N(k-sp)	7,683	1,647	12,899
N(anc)	322,997	129,895	429,963
T(k-sp)	1.85.E+06	1.65.E+06	1.99.E+06
T(h-k/sp)	2.61.E+06	2.14.E+06	4.67.E+06
T(m)	1.42.E+05	7.17.E+04	2.99.E+05
M(k→h)	8.44E–07	4.87E–07	2.30E–06
M(h→k)	1.13E–06	9.71E–07	1.90E–06
Nm(k→h)	0.020	0.012	0.044
Nm(h→k)	0.026	0.021	0.042
M(sp→h)	7.00E–07	4.80E–07	1.08E–06
M(h→sp)	5.47E–08	3.17E–08	6.65E–08
Nm(sp→h)	0.016	0.011	0.020
Nm(h→sp)	0.027	0.014	0.030

N, effective population size in haploid number; Nm, effective number of migrants; T, time; M, migration rate in backward time; h, *Rhododendron keiskei* var. *hypoglaucum*; k, *R. keiskei* var. *keiskei*; sp, *Rhododendron* sp.; anc, ancestral population.

Genetic diversity of local endemics and widespread species. — Compared to widespread species, species with narrow distributions tend to show lower genetic diversity (Frankham & al., 2002; Willi & al., 2022). As expected, the two taxa of *Rhododendron keiskei* var. *hypoglaucum* and *Rhododendron* sp. with limited distributions (Yang & al., 2015; Japanese Ministry of Environment, 2020) exhibited lower expected heterozygosity (0.023/0.008 for var. *hypoglaucum* and 0.020/0.007 for *Rhododendron* sp.; statistics from MIG-seq/GBS), compared to the wide-ranging *R. keiskei* var. *keiskei* (Table 1). The values are representing the lowest levels among other congenic species assessed with genome-wide SNP markers, including endangered species (0.111 in *R. amesiae* [Ao & al., 2022], 0.090 in *R. tsusiophyllum* [Yoichi & al., 2021], 0.074 in *R. meddianum* [Zhang & al., 2021], 0.067 in *R. cyanocarpum* [Liu & al., 2020], 0.053 in *R. kaempferi* and 0.047 in *R. indicum* [Yoichi & al., 2018]). Historical demographic analysis revealed that these taxa had been maintained as small populations (Fig. 5) without receiving a significant number of migrants from the neighboring *R. keiskei* var. *keiskei* (Figs. 2, 4). The historical effective number of migrants was estimated to be only at the order of 10^{-2} (Nm ranged from 0.016 to 0.027, Table 2), and the close parapatric population pairs of *R. keiskei* var. *keiskei* and var. *hypoglaucum* showed no signatures of recent genetic admixture (Figs. 2, 3B). The limited gene flow from the neighboring *R. keiskei* var. *keiskei* populations would be attributed to geographic isolation for *Rhododendron* sp. (Fig. 2) and primarily to ecological barriers for *R. keiskei* var. *hypoglaucum*, which shows differential adaptation to dry and exposed habitat. Such long isolation of local endemics as small populations would have depauperated their genetic diversity (Table 1) via the processes of bottlenecks, random drift, and inbreeding, as seen in the azaleas in some of remote oceanic islands (Isagi & al., 2020).

The southwestern regions of Japan currently have a temperate and mesic climate, which supports dense forests. As a result, *Rhododendron keiskei* var. *keiskei*, which prefers shaded habitats under forest canopy, expands its distribution in the temperate regions of Japanese islands. In the glacial maxima, however, the regions had cooler and drier climates, which resulted in boreal woodlands interspersed with open vegetation (Tsukada, 1983; Hayashi & al., 2010). The harsh climatic conditions during the glacial periods forced temperate plants to retreat to southern coastal refugia (Aoki & al., 2019; Sakaguchi & al., 2021; Tsumura, 2023). The ADMIXTURE and phylogenetic analyses of *R. keiskei* var. *keiskei* populations detected a significant phylogeographic structure, consisting of at least five genetic clusters (Figs. 2A, 3B). The presence of these population groups indicates that *R. keiskei* var. *keiskei* survived unfavorable glacial periods in multiple refugia, which could have enabled var. *keiskei* to maintain high genetic diversity at the species level (Table 1, Fig. 5).

Species delimitation of *Rhododendron keiskei* complex. — As discussed above, the morphologically similar taxa of

Rhododendron keiskei var. *hypoglaucum* and *Rhododendron* sp. would have independently evolved and maintained genetic integrity even under historical gene exchanges, indicating that they represent distinct metapopulation lineages. Additionally, demographic modeling suggests that they do not form a monophyletic group, thus not satisfying the species concept based on monophyly (Donoghue, 1985; De Queiroz, 2007). In addition to genetic evidence, our morphological inspections revealed trait differences between *R. keiskei* var. *hypoglaucum* and *Rhododendron* sp. that were previously unnoticed (Yang & al., 2015). Particularly, the number of flowers developed per inflorescence (var. *hypoglaucum* 1–2 vs. *Rhododendron* sp. 2–6), petiole length and leaf surface structures (stomata, gland scale and epicuticular wax) showed significant differences between the two lineages (Table 3). Based on the combined datasets, *Rhododendron* sp. should be recognized as a distinct species from *R. keiskei* var. *hypoglaucum*. On the other hand, *R. keiskei* var. *hypoglaucum* has been treated as an intraspecific taxon of *R. keiskei* (Suzuki, 1932; Yamazaki, 1996). However, our genetic analysis demonstrated the absence of recent gene flow between *R. keiskei* var. *hypoglaucum* and var. *keiskei* populations, even where their distributions are in contact (Fig. 2). This finding suggests that the two entities are reproductively isolated, providing a strong support to regard them as distinct species. Overall, based on the genetic and morphological differences, the three *Rhododendron* groups are justifiably recognized as independent species. We hereby describe *Rhododendron* sp. as a new species, and raise the taxonomic rank of *R. keiskei* var. *hypoglaucum* to species.

Table 3. Comparison of geographic distribution, habitat, and morphological traits of three *Rhododendron* species.

	R. keiskei var. *keiskei*	*R. keiskei* var. *hypoglaucum* (*R. kantoense* nom. & stat. nov.)	*Rhododendron* sp. (*R. tyaihyonii* sp. nov.; formerly identified as var. *hypoglaucum*)
Distribution	Central and western Honshu, Shikoku, Kyushu, Yaku Island, Japan	Kanto District of central Honshu (Tochigi, Gunma, Saitama, Tokyo), Japan	Samseon-myeon, Yeosu, South Korea
Habitat	Shaded rocky slope in mesic forest	Rocky mountain ridge of limestone or chert	Rocky slope in coastal area
Tree height	1–2 m	0.3–1 m	0.3–0.5 m
No. of flowers per inflorescence	2–4	1–2	2–6
Corolla	Pale yellow	White tinged with yellow	White tinged with yellow
Leaves, lamina	Oblong or oblong-lanceolate 3–9 cm long, 0.8–2.0 cm wide, acuminate at apex, pale greenish beneath; thin-coriaceous	Elliptic, elliptic-oblong 2–6 cm long, 1.0–2.7 cm wide, obtuse or subobtuse at apex, glaucous beneath; coriaceous	Elliptic to elliptic-oblong 2–5.5 cm long, 1–2.5 cm wide, obtuse or subacute at apex, glaucous beneath; coriaceous
Leaves, abaxial side			
Cell arrangement	Irregular	Regular	Irregular
Anticlinal wall	Sinuate	Curved	Straight/curved
Periclinal wall	Slightly convex, smooth	Convex, smooth	Slightly convex, smooth
Stomata type	Actinocytic	Actinocytic	Anomocytic
Stomata length (μm)	22.65 ± 2.95	20.34 ± 2.24	16.32 ± 1.86
Stomata width (μm)	21.34 ± 2.42	19.28 ± 3.81	13.47 ± 1.75
Gland scale density (no./mm^2)	2.25 ± 1.29	17.75 ± 3.03	33.15 ± 2.47
Gland scale diameter (μm)	208.87 ± 14.7	158.99 ± 18.3	181.65 ± 14.8
Epicuticular wax	Absent	Rods and filaments	Absent
Leaves, adaxial side			
Cell arrangement	Regular	Regular	Regular
Anticlinal wall	Straight/curved	Straight/curved	Straight/curved
Periclinal wall	Convex, smooth	Slightly convex, smooth	Convex, smooth
Gland scale density (no./mm^2)	0.37 ± 0.48	1.75 ± 1.2	5.87 ± 0.78
Gland scale diameter (μm)	203.37 ± 16.43	161.64 ± 22.16	168.21 ± 9.62
Leaves, petiole (mm)	2–10	1–3	4–7

■ TAXONOMIC TREATMENT

Rhododendron tyaihyonii S.Sakag., H.J.Choi & S.C.Kim, **sp. nov.** – Holotype: SOUTH KOREA. Jeollanam-do, Yeosu-si, Samseon-myeon, Dongdo-ri, Daesambudo Isl., 15 Apr 2015, *J.C. Yang 15041501* (KH barcode KHB 1624377! [fl.]; isotypes: KH barcodes KHB1624378! [fl.], KHB1624376!, KYO barcode KYO 00029270!, SKK barcode SKK064616!).

Description. – Dwarf evergreen shrubs 0.3–0.5 m (rarely 2 m). Lepidote hairs entire. Leaves elliptic to elliptic-oblong, 2–5.5 cm long, 1–2.5 cm wide, obtuse or subacute at apex, glaucous beneath, coriaceous. Abaxial, irregular cell arrangement, stomata anomocytic, 16.32 ± 1.86 µm long, 13.47 ± 1.75 µm wide, glandular scale density 33.15 ± 2.47/mm^2, glandular scale diameter 181.65 ± 14.8 µm, epicuticular wax absent. Adaxial, glandular scale density 5.87 ± 0.78/mm^2, glandular scale diameter 168.21 ± 9.62 µm. Petiole 4–7 mm long. Flower-bud terminal, single (rarely 2–3), oblong-ovate. Inflorescences umbel-like racemes, with 2–6 flowers. Corolla white tinged with yellow, funnel-shaped, ca. 2.5 long, 3 cm wide, sparsely lepidote outside. Stamens 10–12, irregular, similar or slightly longer than corolla. Ovary oblong-lanceolate, densely lepidote. Style slightly curved, longer than corolla, glabrous. Capsule cylindric, straight, 10–13 mm long, 2–3 mm wide, densely lepidote. Seeds oblong, ca. 1 mm long, with a short appendage on another side. [Illustration and photographs of this plant are provided in Yang & al. (2015).]

Distribution. – SOUTH KOREA. Jeollanam-do, Yeosu-si, Samseon-myeon. Narrowly endemic to Daesambudo Island.

Ecology. – The plants are found on the northern slope of Daesambudo Island. They inhabit coastal rocky places with the evergreen woody species of *Rhaphiolepis indica* var. *umbellata* (Thunb.) H.Ohashi, *Ligustrum japonicum* Thunb., *Camellia japonica* L, *Litsea japonica* (Thunb.) Juss.

Etymology. – The specific epithet, "*tyaihyonii*", is named in honor of Chung Tyaihyon (1883–1971), known as the father of plant taxonomy in Korea and the first curator of Sungkyunkwan University Herbarium (Ha Eun Herbarium, SKK). We have a better understanding of Korean flora thanks to his work in the early to mid-1900s.

Korean name. – Seom-Jin-Dal-Rae.

Japanese name. – Chosen-Hikage-Tsutsuji.

English name. – Tyaihyon's rhododendron.

Additional specimens examined. – SOUTH KOREA. Jeollanam-do, Yeosu-si, Samseon-myeon, Dongdo-ri, Daesambudo Isl., 16 May 2012, *S.J. Ji 12051401* (KH barcodes KHB1624373, KHB1624374, KHB1624375).

Rhododendron kantoense S.Sakag. & Y.Watan., **nom. & stat. nov.** ≡ *Rhododendron keiskei* var. *hypoglaucum* Suto & T.Suzuki in Trans. Nat. Hist. Soc. Formosa 22: 23. 1932 – Holotype: JAPAN. Kanto District, Tochigi (Shimotsuke), Kanuma, Mt. Ozaku, 1 May 1931, *E. Kitamura ST3902* (TAI barcode TAI 119040 [image!] [fl.]; isotype: TNS barcode TNS 55292 [image!]).

Note. – *Rhododendron kantoense* is similar to *R. tyaihyonii*, the differences being: the latter has petiole 4–7 mm long; stomata type anomocytic; inflorescence with 2–6 flowers.

Distribution. – JAPAN. Kanto, Prefectures of Tochigi, Gunma, Saitama and Tokyo. Endemic to the chert and limestone mountain ridges of Kanto District.

Etymology. – The specific epithet "*kantoense*" is derived from the Kanto District, where this species is distributed.

Japanese name. – Urajiro-Hikage-Tsutsuji.

Korean name. – Il-bon-Huin-Jin-Dal-Rae.

English name. – Kanto rhododendron.

Additional specimens examined. – JAPAN. **Gunma Pref.,** Tano-gun, 14 Nov 1982, *S. Kato s.n.* (SMNH 23691); Tano-gun, 14 Oct 1985, *T. Iwata s.n.* (SMNH 14588); Tano-gun, 24 Aug 1975, *T. Satomi s.n.* (OSA 22953). **Saitama Pref.,** Chichibu, 6 Apr 1966, *T. Iwata s.n.* (SMNH 14584); Chichibu, 14 Apr 1968, *T. Moriya s.n.* (TNS 223185); Chichibu, 7 Apr 1971, *T. Iwata s.n.* (SMNH 14585); Chichibu, 15 May 1975, *T. Iwata s.n.* (SMNH 14586); Chichibu, 9 May 1976, *T. Iwata s.n.* (SMNH 14587). **Tochigi Pref.,** Kanuma, 28 Apr 1970, *J. Haginiwa s.n.* (TNS 970427, TNS 970428, TNS 970429, TNS 970430, TNS 970431, TNS 970432, TNS 970433, TNS 970434, TNS 971460, TNS 984648); Kamitsuga-gun, 17 Jul 1962, *T. Matsuzawa s.n.* (TNS 153183). **Tokyo Metropolis,** Nishitama-gun, 21 Jul 1993, *K. Suzuki s.n.* (MAK 272328).

Key to the *Rhododendron keiskei* complex

1. Corolla yellow 2
1. Corolla white tinged with yellow 3
2. Leaves oblong or oblong-lanceolate, apex acuminate, 3–9 cm long, 0.8–2 cm wide, pale greenish beneath ..... ***R. keiskei***
2. Leaves elliptic, apex obtuse to subacute, 1.5–2.5 cm long, 1.0–1.5 wide, pale glaucous beneath ..... ***R. keiskei*** var. ***ozawae***
3. Flowers per inflorescence 1–2, petiole 1–3 mm long, stomata type actinocytic ..... ***R. kantoense***
3. Flowers per inflorescence 2–6, petiole 4–7 mm long, stomata type anomocytic ..... ***R. tyaihyonii***

■ DATA AVAILABILITY

The MIG-seq reads are deposited in the DRA of DDBJ with the following accession numbers: DRR524432–DRR524531. For GBS, the BioSample accession numbers of SAMN39398661–39398666 under BioProject number of PRJNA1063540 were deposited in the NCBI database.

■ AUTHOR CONTRIBUTIONS

SS, HJC and SCK conceived and designed the research. SS, HJC, WY, DT, MM, SM, TH, NK, YK, HJC and SCK collected plant materials. SS, HJC and SKH performed genetic experiments. JHS investigated leaf morphology using SEM. SS led the manuscript writing, with inputs from all authors.

■ ACKNOWLEDGMENTS

This study was financially supported by the Korea National Arboretum (KNA1-1-18, 15-3), Korea Basic Science Institute (National Research Facilities and Equipment Center) grant funded by the Ministry of Education (2023R1A6C101B022), and by Japan Society for the Promotion of Science KAKENHI Grant Number 24H00055. Korea National Arboretum and Daegu Arboretum are acknowledged for providing plant materials of *Rhododendron tyaihyonii*. Drs. S. Fujii, T. Yamashiro, and T. Ohmori are acknowledged for their assistance in collecting plant materials. We are grateful to Dr. D.-C. Son for his valuable comments on taxonomic treatments of the *Rhododendron* species, and to Dr. J.-C. Yang for kindly providing a photograph of *R. tyaihyonii*, which is represented in Fig. 1. We express our gratitude to Drs. M. Yokogawa and K. Kiyama for providing the information on specimens deposited in OSA and SMNH.

■ LITERATURE CITED

Abràmoff, M.D., Magalhães, P.J. & Ram, S.J. 2004. Image processing with ImageJ. *Biophotonics Int*. 11: 36–42.

Alexander, D.H., Novembre, J. & Lange, K. 2009. Fast model-based estimation of ancestry in unrelated individuals. *Genome Res.* 19: 1655–1664. https://doi.org/10.1101/gr.094052.109

Ao, Y.S., Chang, Y.H., Liu, D.T., Liu, Y.B. & Ma, Y.P. 2022. Does the critically endangered *Rhododendron amesiae* deserve top priority for conservation? *Pl. Diversity* 44: 625–628. https://doi.org/10.1016/j.pld.2022.09.005

Aoki, K., Tamaki, I., Nakao, K., Ueno, S., Kamijo, T., Setoguchi, H., Murakami, N., Kato, M. & Tsumura, Y. 2019. Approximate Bayesian computation analysis of EST-associated microsatellites indicates that the broadleaved evergreen tree *Castanopsis sieboldii* survived the Last Glacial Maximum in multiple refugia in Japan. *Heredity* 122: 326–340. https://doi.org/10.1038/s41437-018-0123-9

Bolger, A.M., Lohse, M. & Usadel, B. 2014. Trimmomatic: A flexible trimmer for Illumina sequence data. *Bioinformatics* 30: 2114–2120. https://doi.org/10.1093/bioinformatics/btu170

Carstens, B.C., Pelletier, T.A., Reid, N.M. & Satler, J.D. 2013. How to fail at species delimitation. *Molec. Ecol.* 22: 4369–4383. https://doi.org/10.1111/mec.12413

Choi, B., Kim, H., Byun, H.-J., Gang, G.-H., Lee, Y., Myeong, H.-H., So, S. & Jang, T.-S. 2022. A study of the chromosome number and genome size of the rare species *Rhododendron keiskei* var. *hypoglaucum* in Korea. *Korean J. Pl. Taxon.* 52: 102–107. https://doi.org/10.11110/kjpt.2022.52.2.102

Cox, M.P., Peterson, D.A. & Biggs, P.J. 2010. SolexaQA: At-a-glance quality assessment of Illumina second-generation sequencing data. *B. M. C. Bioinf.* 11: 485. https://doi.org/10.1186/1471-2105-11-485

Dayrat, B. 2005. Towards integrative taxonomy. *Biol. J. Linn. Soc.* 85: 407–417. https://doi.org/10.1111/j.1095-8312.2005.00503.x

De Queiroz, K. 2007. Species concepts and species delimitation. *Syst. Biol.* 56: 879–886. https://doi.org/10.1080/10635150701701083

Donoghue, M.J. 1985. A critique of the biological species concept and recommendations for a phylogenetic alternative. *Bryologist* 88: 172–181. https://doi.org/10.2307/3243026

Elshire, R.J., Glaubitz, J.C., Sun, Q., Poland, J.A., Kawamoto, K., Buckler, E.S. & Mitchell, S.E. 2011. A robust, simple genotyping-by-sequencing (GBS) approach for high diversity species. *PLoS ONE* 6: e19379. https://doi.org/10.1371/journal.pone.0019379

Excoffier, L., Marchi, N., Marques, D.A., Matthey-Doret, R., Gouy, A. & Sousa, V.C. 2021. fastsimcoal2: Demographic inference under complex evolutionary scenarios. *Bioinformatics* 37: 4882–4885. https://doi.org/10.1093/bioinformatics/btab468

Frankham, R., Briscoe, D.A. & Ballou, J.D. 2002. *Introduction to conservation genetics*. Cambridge, U.K.: Cambridge University Press. https://doi.org/10.1017/CBO9780511808999

Fraser, D.J. & Bernatchez, L. 2001. Adaptive evolutionary conservation: Towards a unified concept for defining conservation units. *Molec. Ecol.* 10: 2741–2752. https://doi.org/10.1046/j.1365-294X.2001.t01-1-01411.x

Goldstein, P.Z. & DeSalle, R. 2011. Integrating DNA barcode data and taxonomic practice: Determination, discovery, and description. *BioEssays* 33: 135–147. https://doi.org/10.1002/bies.201000036

Hayashi, R., Takahara, H., Hayashida, A. & Takemura, K. 2010. Millennial-scale vegetation changes during the last 40,000 yr based on a pollen record from Lake Biwa, Japan. *Quatern. Res.* 74: 91–99. https://doi.org/10.1016/j.yqres.2010.04.008

Hedrick, P.W. 2009. Conservation genetics and North American bison (*Bison bison*). *J. Heredity* 100: 411–420. https://doi.org/10.1093/jhered/esp024

Hillis, D.M., Chambers, E.A. & Devitt, T.J. 2021. Contemporary methods and evidence for species delimitation. *Ichthyol. & Herpetol.* 109: 895–903. https://doi.org/10.1643/h2021082

Hoang, D.T., Chernomor, O., von Haeseler, A., Minh, B.Q. & Vinh, L.S. 2017. UFBoot2: Improving the ultrafast bootstrap approximation. *Molec. Biol. Evol.* 35: 518–522. https://doi.org/10.1093/molbev/msx281

Hofmeister, B.T., Denkena, J., Colomé-Tatché, M., Shahryary, Y., Hazarika, R., Grimwood, J., Mamidi, S., Jenkins, J., Grabowski, P.P., Sreedasyam, A., Shu, S., Barry, K., Lail, K., Adam, C., Lipzen, A., Sorek, R., Kudrna, D., Talag, J., Wing, R., Hall, D.W., Jacobsen, D., Tuskan, G.A., Schmutz, J., Johannes, F. & Schmitz, R.J. 2020. A genome assembly and the somatic genetic and epigenetic mutation rate in a wild long-lived perennial *Populus trichocarpa*. *Genome Biol.* 21: 259. https://doi.org/10.1186/s13059-020-02162-5

Honda, A., Murakami, S., Harada, M., Tsuchiya, K., Kinoshita, G. & Suzuki, H. 2019. Late Pleistocene climate change and population dynamics of Japanese *Myodes* voles inferred from mitochondrial cytochrome b sequences. *J. Mammalogy* 100: 1156–1168. https://doi.org/10.1093/jmammal/gyz093

Isagi, Y., Makino, T., Hamabata, T., Cao, P.-L., Narita, S., Komaki, Y., Kurita, K., Naiki, A., Kameyama, Y., Kondo, T. & Shibabayashi, M. 2020. Significant loss of genetic diversity and accumulation of deleterious genetic variation in a critically endangered azalea species, *Rhododendron boninense*, growing on the Bonin Islands. *Pl. Spec. Biol.* 35: 166–174. https://doi.org/10.1111/1442-1984.12270

Japanese Ministry of Environment 2020. *Kankyo-sho Red List 2020*. [in Japanese] https://www.env.go.jp/content/900515981.pdf

Joffard, N., Buatois, B., Arnal, V., Véla, E., Montgelard, C. & Schatz, B. 2022. Delimiting species in the taxonomically challenging orchid section *Pseudophrys*: Bayesian analyses of genetic and phenotypic data. *Frontiers Ecol. Evol.* 10: 1058550. https://doi.org/10.3389/fevo.2022.1058550

Kalyaanamoorthy, S., Minh, B.Q., Wong, T.K.F., von Haeseler, A. & Jermiin, L.S. 2017. ModelFinder: Fast model selection for accurate phylogenetic estimates. *Nature Meth.* 14: 587–589. https://doi.org/10.1038/nmeth.4285

Kikuchi, S. & Osone, Y. 2021. Subspecies divergence and pronounced phylogenetic incongruence in the East-Asia-endemic shrub *Magnolia sieboldii*. *Ann. Bot. (Oxford)* 127: 75–90. https://doi.org/10.1093/aob/mcaa174

Kimura, M. 1996. Quaternary paleogeography of the Ryukyu arc. *J. Geogr. (Tokyo)* 105: 259–285. https://doi.org/10.5026/jgeography.105.3_259

Kitamura, A. & Kimoto, K. 2006. History of the inflow of the warm Tsushima Current into the Sea of Japan between 3.5 and 0.8 Ma. *Palaeogeogr. Palaeoclimatol. Palaeoecol.* 236: 355–366. https://doi.org/10.1016/j.palaeo.2005.11.015

Liu, D., Zhang, L., Wang, J. & Ma, Y. 2020. Conservation genomics of a threatened *Rhododendron*: Contrasting patterns of population structure revealed from neutral and selected SNPs. *Frontiers Genet.* 11: 757. https://doi.org/10.3389/fgene.2020.00757

Liu, X. & Fu, Y.-X. 2020. Stairway Plot 2: Demographic history inference with folded SNP frequency spectra. *Genome Biol.* 21: 280. https://doi.org/10.1186/s13059-020-02196-9

Martin, M. 2011. Cutadapt removes adapter sequences from high-throughput sequencing reads. *EMBnet.journal* 17(1): 10–12. https://doi.org/10.4806/ej.17.1.200

Martínez-Domínguez, L., Nicolalde-Morejón, F., Vergara-Silva, F. & Stevenson, D.W. 2024. A review of taxonomic concepts and species delimitation in Cycadales. *Bot. Rev. (Lancaster)* 90: 33–66. https://doi.org/10.1007/s12229-023-09293-x

Mayr, E. 1942. *Systematics and the origin of species, from the viewpoint of a zoologist*. Cambridge, MA: Harvard University Press.

Mayr, E. 1963. *Animal species and evolution*. Cambridge, MA: Harvard University Press. https://doi.org/10.4159/harvard.9780674865327

Minh, B.Q., Schmidt, H.A., Chernomor, O., Schrempf, D., Woodhams, M.D., von Haeseler, A. & Lanfear, R. 2020. IQ-TREE 2: New models and efficient methods for phylogenetic inference in the genomic era. *Molec. Biol. Evol.* 37: 1530–1534. https://doi.org/10.1093/molbev/msaa015

Momigliano, P., Florin, A.-B. & Merilä, J. 2021. Biases in demographic modeling affect our understanding of recent divergence. *Molec. Biol. Evol.* 38: 2967–2985. https://doi.org/10.1093/molbev/msab047

Morrison, D.A. 2017. Species concepts in biology: Historical development, theoretical foundations and practical relevance.—By Frank E. Zachos. *Syst. Biol.* 67: 177–180. https://doi.org/10.1093/sysbio/syw109

Murray, M.G. & Thompson, W.F. 1980. Rapid isolation of high molecular weight plant DNA. *Nucl. Acids Res.* 8: 4321–4325. https://doi.org/10.1093/nar/8.19.4321

Oksanen, J., Blanchet, F.G., Kindt, R., Legendre, P., Minchin, P.R., O'Hara, R.B., Simpson, G.L., Solymos, P., Henry, M., Stevens, H. & Wagner, H. 2012. vegan: Community Ecology Package. Version 2.5-6. https://cran.r-project.org/web/packages/vegan/index.html

Ossowski, S., Schneeberger, K., Lucas-Lledó, J.I., Warthmann, N., Clark, R.M., Shaw, R.G., Weigel, D. & Lynch, M. 2010. The rate and molecular spectrum of spontaneous mutations in *Arabidopsis thaliana*. *Science* 327: 92–94. https://doi.org/10.1126/science.1180677

Padilla-García, N., Rojas-Andrés, B.M., López-González, N., Castro, M., Castro, S., Loureiro, J., Albach, D.C., Machon, N. & Martínez-Ortega, M.M. 2018. The challenge of species delimitation in the diploid-polyploid complex *Veronica* subsection *Pentasepalae*. *Molec. Phylogen. Evol.* 119: 196–209. https://doi.org/10.1016/j.ympev.2017.11.007

Poorter, H., Niinemets, Ü., Poorter, L., Wright, I.J. & Villar, R. 2009. Causes and consequences of variation in leaf mass per area (LMA): A meta-analysis. *New Phytol.* 182: 565–588. https://doi.org/10.1111/j.1469-8137.2009.02830.x

Pritchard, J.K., Stephens, M. & Donnelly, P. 2000. Inference of population structure using multilocus genotype data. *Genetics* 155: 945–959. https://doi.org/10.1093/genetics/155.2.945

Qiu, Y.X., Sun, Y., Zhang, X.P., Lee, J., Fu, C.X. & Comes, H.P. 2009. Molecular phylogeography of East Asian *Kirengeshoma* (Hydrangeaceae) in relation to Quaternary climate change and landbridge configurations. *New Phytol.* 183: 480–495. https://doi.org/10.1111/j.1469-8137.2009.02876.x

R Development Core Team 2018. R: A language and environment for statistical computing. Version 3.5.0. Vienna: R Foundation for Statistical Computing. https://cran-archive.r-project.org/bin/windows/base/old/3.5.0/

Rochette, N.C., Rivera-Colón, A.G. & Catchen, J.M. 2019. Stacks 2: Analytical methods for paired-end sequencing improve RADseq-based population genomics. *Molec. Ecol.* 28: 4737–4754. https://doi.org/10.1111/mec.15253

Roesti, M., Gavrilets, S., Hendry, A.P., Salzburger, W. & Berner, D. 2014. The genomic signature of parallel adaptation from shared genetic variation. *Molec. Ecol.* 23: 3944–3956. https://doi.org/10.1111/mec.12720

Sakaguchi, S., Qiu, Y.-X., Liu, Y.-H., Qi, X.-S., Kim, S.-H., Han, J., Takeuchi, Y., Worth, J.R.P., Yamasaki, M., Sakurai, S. & Isagi, Y. 2012. Climate oscillation during the Quaternary associated with landscape heterogeneity promoted allopatric lineage divergence of a temperate tree *Kalopanax septemlobus* (Araliaceae) in East Asia. *Molec. Ecol.* 21: 3823–3838. https://doi.org/10.1111/j.1365-294X.2012.05652.x

Sakaguchi, S., Kimura, T., Kyan, R., Maki, M., Nishino, T., Ishikawa, N., Nagano, A.J., Honjo, M.N., Yasugi, M., Kudoh, H., Li, P., Choi, H.J., Chernyagina, O.A. & Ito, M. 2018. Phylogeographic analysis of the East Asian goldenrod (*Solidago virgaurea* complex, Asteraceae) reveals hidden ecological diversification with recurrent formation of ecotypes. *Ann. Bot. (Oxford)* 121: 489–500. https://doi.org/10.1093/aob/mcx182

Sakaguchi, S., Asaoka, Y., Takahashi, D., Isagi, Y., Imai, R., Nagano, A.J., Qiu, Y.X., Li, P., Lu, R. & Setoguchi, H. 2021. Inferring historical survivals of climate relicts: The effects of climate changes, geography, and population-specific factors on herbaceous hydrangeas. *Heredity* 126: 615–629. https://doi.org/10.1038/s41437-020-00396-4

Schluter, D. & Nagel, L.M. 1995. Parallel speciation by natural selection. *Amer. Naturalist* 146: 292–301. https://doi.org/10.1086/285799

Schmid-Siegert, E., Sarkar, N., Iseli, C., Calderon, S., Gouhier-Darimont, C., Chrast, J., Cattaneo, P., Schütz, F., Farinelli, L., Pagni, M., Schneider, M., Voumard, J., Jaboyedoff, M., Fankhauser, C., Hardtke, C.S., Keller, L., Pannell, J.R., Reymond, A., Robinson-Rechavi, M., Xenarios, I. & Reymond, P. 2017. Low number of fixed somatic mutations in a long-lived oak tree. *Nature Plants* 3: 926–929. https://doi.org/10.1038/s41477-017-0066-9

Supple, M.A. & Shapiro, B. 2018. Conservation of biodiversity in the genomics era. *Genome Biol.* 19: 131. https://doi.org/10.1186/s13059-018-1520-3

Suyama, Y. & Matsuki, Y. 2015. MIG-seq: An effective PCR-based method for genome-wide single-nucleotide polymorphism genotyping using the next-generation sequencing platform. *Sci. Rep.* 5: 16963. https://doi.org/10.1038/srep16963

Suyama, Y., Hirota, S.K., Matsuo, A., Tsunamoto, Y., Mitsuyuki, C., Shimura, A. & Okano, K. 2022. Complementary combination of multiplex high-throughput DNA sequencing for molecular phylogeny. *Ecol. Res.* 37: 171–181. https://doi.org/10.1111/1440-1703.12270

Suzuki, T. 1932. A new variety of *Rhododendron keiskei* Miq. *Trans. Nat. Hist. Soc. Formosa* 22: 118–119.

Tsukada, M. 1983. Vegetation and climate during the Last Glacial Maximum in Japan. *Quatern. Res.* 19: 212–235. https://doi.org/10.1016/0033-5894(83)90006-6

Tsumura, Y. 2023. Review: Genetic structure and local adaptation in natural forests of *Cryptomeria japonica*. *Ecol. Res.* 38: 64–73. https://doi.org/10.1111/1440-1703.12320

Wang, M.-Z., Wu, J., Zhang, S.-L., Mao, L.-M., Ohi-Toma, T., Takano, A., Zhang, Y.-H., Cameron, K.M. & Li, P. 2024. Species delimitation in *Amana* (Liliaceae): Transcriptomes battle with evolutionary complexity. *Cladistics* 40: 135–156. https://doi.org/10.1111/cla.12565

Waples, R.S., Kays, R., Fredrickson, R.J., Pacifici, K. & Mills, L.S. 2018. Is the red wolf a listable unit under the US Endangered Species Act? *J. Heredity* 109: 585–597. https://doi.org/10.1093/jhered/esy020

Willi, Y., Kristensen, T.N., Sgrò, C.M., Weeks, A.R., Ørsted, M. & Hoffmann, A.A. 2022. Conservation genetics as a management tool: The five best-supported paradigms to assist the management of threatened species. *Proc. Natl. Acad. Sci. U.S.A.* 119: e2105076119. https://doi.org/10.1073/pnas.2105076119

Wu, Y., Hipp, A.L., Fargo, G., Stith, N. & Ricklefs, R.E. 2023. Improving species delimitation for effective conservation: A case study in the endemic maple-leaf oak (*Quercus acerifolia*). *New Phytol.* 238: 1278–1293. https://doi.org/10.1111/nph.18777

Yamazaki, T. 1996. *A revision of the genus Rhododendron in Japan, Taiwan, Korea and Sakhalin*. Tokyo: Tsumura Laboratory.

Yang, J.-C., Kwon, Y.-H., Ji, S.-J. & Shin, C.-H. 2015. A new record of *Rhododendron keiskei* Miq. var. *hypoglaucum* Suto & Suzuki (Ericaceae) in Korea. *Korean J. Pl. Taxon.* 45: 239–242. https://doi.org/10.11110/kjpt.2015.45.3.239

Yang, Z. 2015. The BPP program for species tree estimation and species delimitation. *Curr. Zool.* 61: 854–865. https://doi.org/10.1093/czoolo/61.5.854

Yoichi, W., Kawamata, I., Matsuki, Y., Suyama, Y., Uehara, K. & Ito, M. 2018. Phylogeographic analysis suggests two origins for the riparian azalea *Rhododendron indicum* (L.) Sweet. *Heredity* 121: 594–604. https://doi.org/10.1038/s41437-018-0064-3

Yoichi, W., Takahashi, M., Nagano, A.J., Uehara, K. & Abe, H. 2021. Evolutionary effects of geographic and climatic isolation between *Rhododendron tsusiophyllum* populations on the Izu Islands and mainland Honshu of Japan. *Heredity* 126: 859–868. https://doi.org/10.1038/s41437-021-00417-w

Zachos, F.E. 2015. Taxonomic inflation, the phylogenetic species concept and lineages in the tree of life – A cautionary comment on species splitting. *J. Zool. Syst. Evol. Res.* 53: 180–184. https://doi.org/10.1111/jzs.12088

Zhang, C., Meng, R., Meng, Y., Guo, B.-L., Liu, Q.-R. & Nie, Z.-L. 2023. Parallel evolution, atavism, and extensive introgression explain the radiation of *Epimedium* sect. *Diphyllon* (Berberidaceae) in southern East Asia. *Frontiers Pl. Sci. (Lausanne)* 14: 1234148. https://doi.org/10.3389/fpls.2023.1234148

Zhang, X.-J., Liu, X.-F., Liu, D.-T., Cao, Y.-R., Li, Z.-H., Ma, Y.-P. & Ma, H. 2021. Genetic diversity and structure of *Rhododendron meddianum*, a plant species with extremely small populations. *Pl. Diversity* 43: 472–479. https://doi.org/10.1016/j.pld.2021.05.005

Appendix 1. List of taxa sampled with information related to taxonomy (species name), voucher information (see suppl. Table S2), and GenBank accession numbers.

Rhododendron albrechtii Maxim., Japan: Nagano, *Kurata, S. 32184* (KAG), DRR524530, DRR524531; ***Rhododendron kantoense*** S.Sakag. & Y.Watan., nom. & stat. nov., Japan: Tokyo, *Suzuki, K. 272328* (MAK), DRR524459; Tochigi, *Haginiwa, J. 970427* (TNS), DRR524506, DRR524507, DRR524508, DRR524509, DRR524510, DRR524511, DRR524512, DRR524513, DRR524514, DRR524515; Gunma, *Kato, S. 23691* (SMNH), DRR524516, DRR524517, DRR524518, DRR524519, DRR524520, DRR524521, DRR524522, DRR524523, DRR524524, DRR524525; ***Rhododendron keiskei*** Miq., Japan: Aichi, Shinshiro, *Fujii, S. 16916* (KYO), DRR524481, Aichi, Shinshiro, *Togashi, N. 436340* (TNS), DRR524526, DRR524527; Ehime, Kamiukena-gun, *Kobayashi, T. 40800* (KYO), DRR524472; Ehime, Kamiukena-gun, *Ito, H. 1074016* (TNS), DRR524493, DRR524494, DRR524495; Gifu, Mino, *Takahashi, H. 671838* (TNS), DRR524485, DRR524486, DRR524487; Gunma, Ueno, *Watanabe, Y. 27121* (KYO), DRR524501, DRR524502, DRR524503, DRR524504, DRR524505; Hyogo, Himeji, *Maruoka, M. 1294290* (TNS), DRR524488, DRR524489, DRR524490; Hyogo, Kanzaki, *Kobayashi, T. 43154* (KYO), DRR524475; Hyogo, Sasayama, *Kobayashi, T. 58017* (KYO), DRR524484; Kagoshima, Kirishima, *Kawagoe, S. 32589* (KAG), DRR524455, DRR524456; *Naito, T. 32590* (KAG), DRR524460, DRR524461; Kagoshima, Kumage-gun, *Hatsushima, S. 32571* (KAG), DRR524457, DRR524458; Kyoto, Kyoto, *Nakatsukasa, A. 18* (KYO), DRR524473; Kyoto, Nantan, *Tsugaru, S. & Takagi, H. 487954* (TNS), DRR524434, DRR524435; Miyazaki, Nishiusuki-gun, *Hatsushima, S. 32554* (KAG), DRR524462, DRR524463, DRR52446, DRR524467, DRR524468, DRR524469, DRR524470, DRR524471; Nagasaki, Omura, *Tashiro, Z. 31179* (TNS), DRR524465, DRR524466; Nara, Yoshino-gun, *Morimoto, N. 9868* (KYO), DRR524477; Nara, Yoshino-gun, *Morimoto, N. 11731* (KYO), DRR524478, DRR524480; Nara, Yoshino-gun, *Kawabata, K. 11306* (KYO), DRR524483, DRR524491, DRR524492; Oita, Saiki, *Kobayashi, T. 44381* (KYO), DRR524476; Shizuoka, Shizuoka, *Yamamoto, S. 23911* (KYO), DRR524436, DRR524437; Tochigi, Kanuma, *Haginiwa, J. 984641* (TNS), DRR524496, DRR524497, DRR524498, DRR524499, DRR524500; Wakayama, Nishimuro-gun, *Noshiro, S. 25488* (KYO), DRR524479; Wakayama, Shingu, *Yamamoto, S. 23911* (KYO), DRR524474; Wakayama, Tanabe, *Noshiro, S. 25352* (KYO), DRR524482; ***Rhododendron mucronulatum*** Turcz. var. *ciliatum* Nakai, Japan: Nagasaki, Tsushima, *Toagshi, M. 330008* (TNS), DRR524528, DRR524529 (voucher missing); ***Rhododendron nipponicum*** Matsum., Japan: Nagano, *Kurata, S. 32775* (KAG), DRR524432, DRR524433; ***Rhododendron tyaihyonii*** S.Sakag., H.J.Choi & S.C.Kim, sp. nov., South Korea: Jeollanam-do, *Yang, J.C. 1624377* (KHB), DRR524438, DRR524439, DRR524440, DRR524441, DRR524442, DRR524443, DRR524444, DRR524445, DRR524446, DRR524447, DRR524448, DRR524449, DRR524450, DRR524451, DRR524452, DRR524453, DRR524454.